

Wide and Deep Exploration of Radio Galaxies with Subaru HSC (WERGS). III.
Discovery of a $z = 4.72$ Radio Galaxy with Lyman Break Technique

TAKUJI YAMASHITA,^{1,2} TOHRU NAGAO,² HIROYUKI IKEDA,^{1,3} YOSHIKI TOBA,^{4,5,2} MASARU KAJISAWA,^{2,6} YOSHIKI ONO,⁷
MASAYUKI TANAKA,¹ MASAYUKI AKIYAMA,⁸ YUICHI HARIKANE,¹ KOHEI ICHIKAWA,^{9,8} TOSHIHIRO KAWAGUCHI,¹⁰
TAIKI KAWAMURO,¹ KOTARO KOHNO,^{11,12} CHIEN-HSIU LEE,¹³ KIANHONG LEE,¹¹ YOSHIKI MATSUOKA,² MANA NIIDA,⁶
KAZUYUKI OGURA,^{14,15} MASAFUSA ONOUE,¹⁶ AND HISAKAZU UCHIYAMA¹

¹*National Astronomical Observatory of Japan, 2-21-1 Osawa, Mitaka, Tokyo 181-8588, Japan*

²*Research Center for Space and Cosmic Evolution, Ehime University, 2-5 Bunkyo-cho, Matsuyama, Ehime 790-8577, Japan*

³*National Institute of Technology, Wakayama College, 77 Noshima, Nada, Gobo, Wakayama 644-0023, Japan*

⁴*Department of Astronomy, Kyoto University, Kitashirakawa-Oiwake-cho, Sakyo-ku, Kyoto 606-8502, Japan*

⁵*Academia Sinica Institute of Astronomy and Astrophysics, 11F of Astronomy-Mathematics Building, AS/NTU, No.1, Section 4, Roosevelt Road, Taipei 10617, Taiwan*

⁶*Graduate School of Science and Engineering, Ehime University, Bunkyo-cho, Matsuyama, Ehime 790-8577, Japan*

⁷*Institute for Cosmic Ray Research, The University of Tokyo, 5-1-5 Kashiwanoha, Kashiwa, Chiba 277-8582, Japan*

⁸*Astronomical Institute, Tohoku University, 6-3 Aramaki, Aoba-ku, Sendai, Miyagi 980-8578, Japan*

⁹*Frontier Research Institute for Interdisciplinary Sciences, Tohoku University, Sendai, Miyagi 980-8578, Japan*

¹⁰*Department of Economics, Management and Information Science, Onomichi City University, Onomichi, Hiroshima 722-8506, Japan*

¹¹*Institute of Astronomy, School of Science, The University of Tokyo, 2-21-1 Osawa, Mitaka, Tokyo 181-0015, Japan*

¹²*Research Center for the Early Universe, The University of Tokyo, 7-3-1 Hongo, Bunkyo, Tokyo 113-0033, Japan*

¹³*National Optical Astronomy Observatory, 950 N. Cherry Ave., Tucson, AZ 85719, USA*

¹⁴*Faculty of Education, Bunkyo University, 3337, Minami-ogishima, Koshigaya, Saitama 343-8511, Japan*

¹⁵*Nishi-Harima Astronomical Observatory, Center for Astronomy, University of Hyogo, 407-2 Nishigaichi, Sayo, Hyogo 679-5313, Japan*

¹⁶*Max-Planck-Institut für Astronomie, Königstuhl 17, D-69117 Heidelberg, Germany*

(Received; Revised; Accepted)

ABSTRACT

We report a discovery of $z = 4.72$ radio galaxy, HSC J083913.17+011308.1, by using the Lyman break technique with the Hyper Suprime-Cam Subaru Strategic Survey (HSC-SSP) catalog for VLA FIRST radio sources. The number of known high- z radio galaxies (HzRGs) at $z > 3$ is quite small to constrain the evolution of HzRGs so far. The deep and wide-area optical survey by HSC-SSP enables us to apply the Lyman break technique to a large search for HzRGs. For an HzRG candidate among pre-selected r -band dropouts with a radio detection, a follow-up optical spectroscopy with GMOS/Gemini has been performed. The obtained spectrum presents a clear Ly α emission line redshifted to $z = 4.72$. The SED fitting analysis with the rest-frame UV and optical photometries suggests the massive nature of this HzRG with $\log M_*/M_\odot = 11.4$. The small equivalent width of Ly α and the moderately red UV colors indicate its dusty host galaxy, implying a chemically evolved and dusty system. The radio spectral index does not meet a criterion for an ultra-steep spectrum: α_{1400}^{325} of -1.1 and α_{1400}^{150} of -0.9 , demonstrating that the HSC-SSP survey compensates for a sub-population of HzRGs which are missed in surveys focusing on an ultra-steep spectral index.

Keywords: galaxies: active — galaxies: high-redshift — radio continuum: galaxies

1. INTRODUCTION

Observations and numerical studies suggest that feedback effects from radio galaxies (RGs) can play a key role on the evolution of galaxies by regulating star formation (e.g., Croton et al. 2006; Wagner, & Bicknell 2011; Fabian 2012; Morganti et al. 2013; McNamara et al. 2005). It is important to describe the number densities of RGs along the cosmic time up to the early Universe

for understanding the evolution of galaxies and active galactic nuclei (AGNs). In particular, high- z RGs (HzRGs) at $z > 2$ represent a key population to reveal the formation of massive galaxies and massive galaxy clusters (Miley & De Breuck 2008), because the stellar mass of HzRGs is typically as massive as $> 10^{11} M_{\odot}$ even at $z > 3$ (Seymour et al. 2007; De Breuck et al. 2010) and the gas metallicity of HzRGs at $z > 3$ exceeds the solar metallicity (Nagao et al. 2006; Matsuoka et al. 2009). The most massive galaxies could be rapidly formed before $z \sim 3$ (e.g., Pérez-González et al. 2008). The number density of RGs moderately increases up to $z \sim 1 - 2$ and is believed to abruptly decline at the HzRG regime at $z = 2 - 3$ (Dunlop & Peacock 1990; Rigby et al. 2015). At $z > 3$, the number density of HzRGs is not well constrained due to a dearth of samples, except a small number of known radio-loud quasars (Bañados et al. 2015).

HzRGs have been historically discovered by using a radio spectral index. HzRGs are empirically known to show an ultra-steep spectrum (USS), which is commonly defined as a spectrum with a radio spectral index α of < -1.3 (De Breuck et al. 2000a; Saxena et al. 2018a, 2019). The USS selection is based on an idea of a steepening radio spectrum with frequency and redshifting (e.g., Carilli & Yun 1999; Morabito & Harwood 2018). The technique using USS was successfully established and is an efficient method to find a lot of HzRGs (De Breuck et al. 2000a). The $z = 5.19$ HzRG, TN J0924–2201, had been discovered with the USS technique and had been the most distant known HzRG record in the past two decades (van Breugel et al. 1999). Recently, Saxena et al. (2018b) broke the redshift record and discovered a $z = 5.72$ HzRG, TGSS J1530+1049, using the USS technique.

However, a small number of $z > 4$ HzRGs without USS has been discovered: non-USS HzRGs at $z = 4.42$ (VLA J123642+621331, Waddington et al. 1999) and $z = 4.88$ (J163912.11+405236.5, Jarvis et al. 2009) were discovered out of radio-detected but very faint objects in optical and near-infrared, respectively. The spectral indices of these two HzRGs are -0.94 between 1.4 GHz and 8.5 GHz and -0.75 between 325 MHz and 1.4 GHz, respectively. Their radio morphologies are compact and must be associated with an AGN. Klammer et al. (2006) indicated that no HzRGs selected based on USS show a curvature in gigahertz spectra. These facts suggest the known HzRGs are a tip of the iceberg. Therefore the true spectral index distribution in HzRGs is unclear. The present biased sample of HzRGs toward USS could lead to misunderstandings of the number density of HzRGs and underlying radio luminosity functions (Jarvis & Rawlings 2000; Jarvis et al. 2001; Yuan et al. 2016, 2017).

Finding HzRGs without relying on the USS technique is now possible by using the Lyman break technique on deep optical imaging (e.g., Steidel et al. 1996).

Great advances of instruments capable deep imaging surveys in wide fields enable us to identify very faint and rare objects such as HzRGs. A search for HzRGs using the Lyman break technique will provide a uniform HzRG sample without biases of radio spectral indices. Hyper Suprime-Cam Subaru Strategic Survey (HSC-SSP, Miyazaki et al. 2018; Aihara et al. 2018a; Komiyama et al. 2018; Kawanomoto et al. 2018; Furusawa et al. 2018) is one of the most suitable programs for this purpose. The Lyman break technique for HSC-SSP photometric objects was successfully applied to search for high- z galaxies (Ono et al. 2018; Harikane et al. 2018; Toshikawa et al. 2018) and high- z quasars (e.g., Akiyama et al. 2018; Matsuoka et al. 2016, 2018a,b, 2019). In this paper, we report a discovery of $z=4.7$ HzRG, HSC J083913.17+011308.1 (hereafter HSC J0839+0113), found out of a pilot survey sample using Subaru HSC and an archival radio catalog. This survey is part of ongoing project, WERGS (Wide and Deep Exploration of RGs with Subaru HSC; Yamashita et al. 2018). This paper is the third in a publication series of WERGS, which follows Yamashita et al. (2018) and Toba et al. (2019) and precedes Ichikawa et al. submitted. Throughout this paper, all magnitudes are presented in the AB system (Oke & Gunn 1983) and are corrected for Galactic extinction (Schlegel et al. 1998). We use the CModel photometry for HSC data (Abazajian et al. 2004). We use a flat Λ CDM cosmological model with $H_0 = 70 \text{ km s}^{-1} \text{ Mpc}^{-1}$, and $\Omega_M = 0.30$. Using this cosmology, at $z = 4.7$ the age of the Universe is 1.2 Gyr and $1''$ corresponds to 6.5 kpc.

2. SELECTION

We utilized the 1.4 GHz radio continuum catalog of the Faint Images of the Radio Sky at Twenty-cm survey (FIRST, Becker et al. 1995) with Very Large Array (VLA). FIRST surveyed the area of the Sloan Digital Sky Survey (SDSS York et al. 2000) and thus entirely covers the HSC-SSP survey fields with a spatial resolution of $5''.4$. We only used radio sources with a peak flux of greater than 1 mJy and a side lobe probability¹ of less than 0.05 in the final release catalog (Helfand et al. 2015).

In order to identify optical counterparts of FIRST sources, we used a forced photometry catalog in the wide-layer of the internally released version, S16A Wide2, of HSC-SSP (Aihara et al. 2018b). The forced photometries were performed for each image using position and shape parameters determined in a reference band. The order of the priority bands as a reference band is *irzyg* according to its signal-to-noise ratio (S/N) approximately (see Bosch et al.

¹ The side lobe probability is a measure of a likelihood that a source is a spurious detection near a bright source.

2018, for more details). Only unique object that has been deblended and photometric based on i -band was selected by flags, `detect_is_primary` and `merge_measurement_i`, in the HSC-SSP database. Further, we imposed the following criteria on objects: in i , r , and z -bands, an object is not affected by cosmic rays (`flags_pixel_cr_center`), not saturated (`flags_pixel_saturated_center`), and not at the edge of a CCD or a coadded image (`flags_pixel_edge` for removing); in i and z -bands, there are no problems in photometries (`cmodel_flux_flags`, `centroid_sdss_flags`); the number of visits at an object position (`countinputs`) is greater than or equal to 4 (6) for the g and r (i and z) bands to ensure a certain observing depth. We have cross-matched between the FIRST sources and the HSC-SSP sources with a search radius of $1''$. This search radius was set to balance between contamination and completeness, where the estimated contamination by chance coincidence is 14% (see Yamashita et al. 2018 for the details).

Out of 4725 matched sources, 16 sources were selected as r -dropouts with $S/N > 5$ in z -band, which meet the following color criteria which are the same ones as those of Ono et al. (2018):

$$r_{AB} - i_{AB} > 1.2 \quad (1)$$

$$i_{AB} - z_{AB} < 0.7 \quad (2)$$

$$r_{AB} - i_{AB} > 1.5(i_{AB} - z_{AB}) + 1.0 \quad (3)$$

The objects further should be not detected in g band or $g_{AB} > r_{AB}$. These r -dropouts are candidates of HzRGs at $z \sim 5$ (Figure 1). HSC J0839+0113 was selected out of them according to the brightness ($z_{AB} < 25$) and the visibility for a follow-up observation with GMOS/Gemini (see the next section). HSC J0839+0113 has a FIRST 1.4 GHz flux of 7.17 ± 0.14 mJy (see also Table 1). Its HSC images and FIRST radio continuum are displayed in Figure 2. The obvious dropout at r -band is seen. The apparent size in the FIRST image is approximately a point source ($\text{FWHM} = 6''.25 \times 5''.30$), as seen in high- z radio sources. There are no other HSC sources within the FIRST beam.

3. SPECTROSCOPIC REDSHIFT AND PHOTOMETRIC DATA

3.1. Spectroscopic Follow-up Observation

A long slit spectroscopy was performed for HSC J0839+0113 using GMOS mounted on the Gemini South telescope on 2018, February 21 (Program ID: GS-2017B-FT-17, PI: T. Yamashita), in order to obtain its spectroscopic redshift. We used the OG515 filter and the R400-G5305 grating blazed at 8300 \AA . The slit width was set to be $1''.0$. The spectral resolution is approximately 8 \AA , which corresponds to 290 km s^{-1} . The spectral coverage was typically $6700 - 10000 \text{ \AA}$. The position angle was set to be 32.56 degree East of North. A total of 7×1030 seconds exposures were obtained.

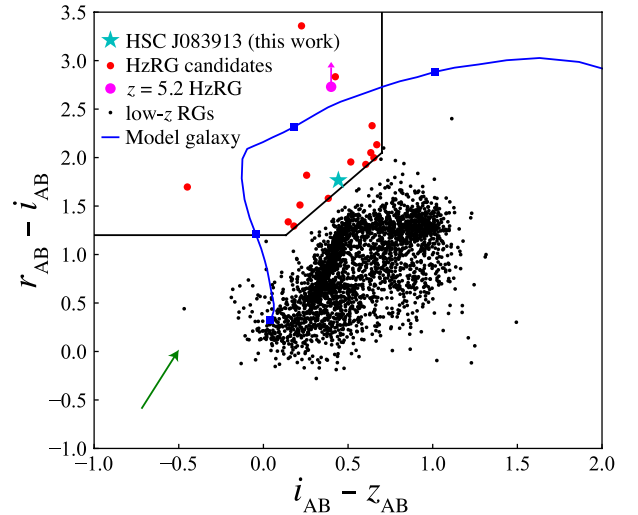


Figure 1. Color-color diagram for selecting HzRG candidates at $z \sim 5$. The candidates are denoted by the red circles and are inside the color selection criteria (black lines, Ono et al. 2018). One candidate is out of the y -axis range. The cyan star represents HSC J0839+0113. The magenta circle denotes the colors of the known HzRG at $z = 5.2$, where used filters were slightly different from HSC’s ones and y -axis is a lower limit (Overzier et al. 2006). The blue line indicates the color track of a star-forming galaxy model produced with a stellar synthesis code of Bruzual & Charlot (2003). The model assumes an instantaneous-burst model with an age of 25 Myr, the solar metallicity, the IGM absorption of Madau (1995), and Lyman α emission with a rest-frame equivalent width of 1180 \AA and an observed frame FWHM of 1530 km s^{-1} (the most large equivalent width case in $z > 2$ HzRGs of Roettgering et al. 1997). The squares on the track mark redshifts of 4.0, 4.5, 5.0, and 5.5. The black dots show low- z RGs in the WERGS sample (Yamashita et al. 2018). The green vector shows the extinction vector of $A_V = 1$ (Calzetti et al. 2000).

Bias frames, flat-fields, CuAr arcs, and standard star Hiltner 600, were also taken for calibration. The seeing of the observation was $0''.99$.

Data reduction was carried out using the Gemini/GMOS IRAF package. Object frames were bias-subtracted and flat-fielded. The wavelength calibration for the object frames was performed using reduced arc frames. After removing cosmic rays, subtracting sky lines, and flux calibration using the spectrophotometric standard star (Hiltner 600), the object frames were combined with median stacking. A 1D spectrum was extracted with an aperture of $1''.9$.

Ly α $\lambda 1216$ emission line is significantly detected at a peak of 6957 \AA in the spectrum (Figure 3). The redshifted Ly α corresponds to a redshift of 4.723 ± 0.001 . The characteristic asymmetric profile of this emission line (see the right panel of Figure 3) and the r -dropout

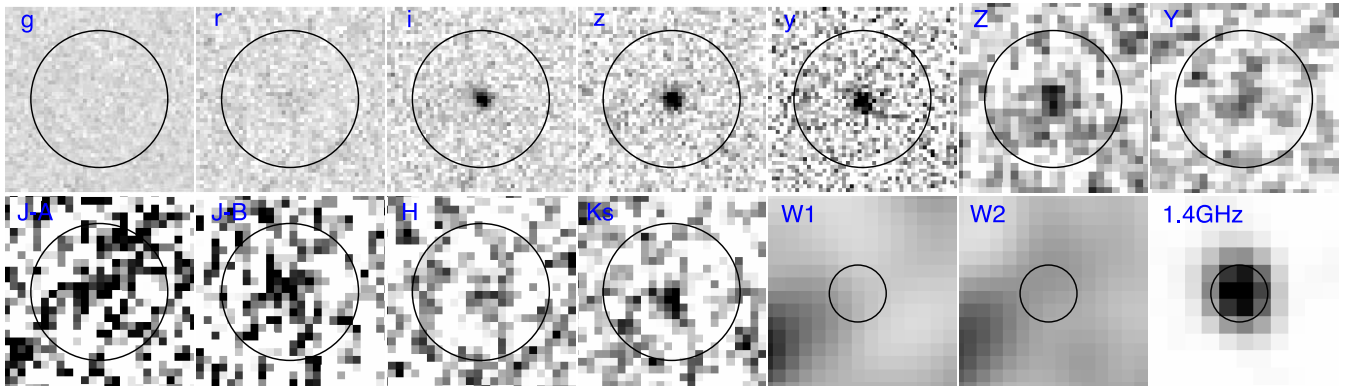


Figure 2. The postage stamp images of HSC J0839+0113. From top left to bottom right, the Subaru HSC *grizy* and VIKING *ZYJHKs* images shown with a width of $8''$, and subsequently the *WISE* *W1W2* and FIRST 1.4 GHz images with a width of $20''$. Two frames of VIKING *J*-band, denoted by *J-A* and *J-B*, respectively, are shown and the results of SED fitting with each *J*-band photometries are discussed in Section 4.2. North is upward and east is to the left. There are no other optical/near-infrared sources within the FIRST detection region (FWHM $\sim 6''$). The infrared counterparts in both *W1* and *W2* are not detected. Circles with an equivalent diameter of $6''$ to the apparent size in the FIRST image serve as a guide to the eye.

of this object credibly support that this line is the redshifted $\text{Ly}\alpha$, although any other lines were not identified in this spectrum. Continuum is also detected at the redder part than the $\text{Ly}\alpha$ line while is not detected in the bluer part, which is consistent with $\text{Ly}\alpha$ break at this redshift. The 2D spectrum shows an extended $\text{Ly}\alpha$ of $1''.3$, which corresponds to 8.4 kpc. This extended $\text{Ly}\alpha$ is approximately equivalent to a deconvolved size of 7.6 kpc in the 1.4 GHz image produced by the FIRST survey project (Helfand et al. 2015).

3.2. SED Fitting Analysis

We estimate a stellar mass of this HzRG by a fitting analysis of its spectral energy distribution (SED). Photometric data of VIKING (Edge et al. 2013) and ALLWISE (Cutri et al. 2014) are available for this object, as well as HSC-SSP (see Figure 2 for images of all bands). Because no entry of this object is in the VIKING DR3 source catalog likely due to its low S/N, we performed aperture photometries on archive VIKING images of all *ZYJHKs*-bands. The VIKING images are convolved to match their PSF to one of *Z*-band, after sky backgrounds are subtracted. The $2''.5$ aperture is used for the object photometries. This aperture radius at the object position encloses an equivalent flux of a *i*-band image convolved to *Z*-band to the CModel *i*-band flux. Therefore the $2''.5$ aperture photometries can measure a total flux of the object. The errors in the photometries are estimated from variations of aperture photometries at object-free regions. Only in *J*-band, two archive image frames are available for this object. We note that two photometry results of these frames are significantly different from each other. This large difference is likely due to an effect from large-scale variations of sky backgrounds on the low S/N images. Thus, we use a weighted mean of the two photometries for the SED fitting anal-

ysis. Finally, we obtain 23.81 (0.03), 23.1 (0.4), 22.6 (0.5), > 22.4 , and 22.4 (0.5) in *ZYJHKs* bands, respectively. The parentheses represent 1σ errors. For a non-detection in *H*-band, the 3σ limit is provided. In ALLWISE, there are no entries in the catalog of both bands of *W1* and *W2*. Even in the images, the object is not detected in both bands, after a possible contamination from an adjacent object is considered (a source at the south-east from HSC J0839+0113 in Figure 2). We thus put 3σ upper limits of $32 \mu\text{Jy}$ and $43 \mu\text{Jy}$ for *W1* and *W2*, respectively.

SED fitting is performed with these optical-to-mid-infrared photometries including upper limits using the CIGALE SED fitting code (Burgarella et al. 2005; Boquien et al. 2019). We basically follow a SED fitting manner of Toba et al. (2019), who applied the CIGALE SED fitting for HSC-selected radio galaxies, but we use somewhat smaller steps of free parameters than Toba et al. (2019) and do not include models of infrared dust emission, radio synchrotron emission, and AGN emission. In our SED fitting analysis, the star formation history of two exponential decreasing star formation with different *e*-folding times is assumed. A stellar template of Bruzual & Charlot (2003) with an initial mass function of Chabrier (2003) is adopted. Dust attenuation is modeled by the dust extinction law of Calzetti et al. (2000). The SED fitting with CIGALE also handle fluxes with upper limits by introducing the error functions for computing χ^2 (see Boquien et al. 2019).

The best-fit SED model is presented in Figure 4. The reduced χ^2 of the best-fit is 0.46 with a degree of freedom of 10. The bayesian-estimated stellar mass is $\log M_*/M_\odot = 11.43_{-0.46}^{+0.22}$, where the super/subscripts are 1σ errors. The mass-weighted age is 230 (160) Myr.

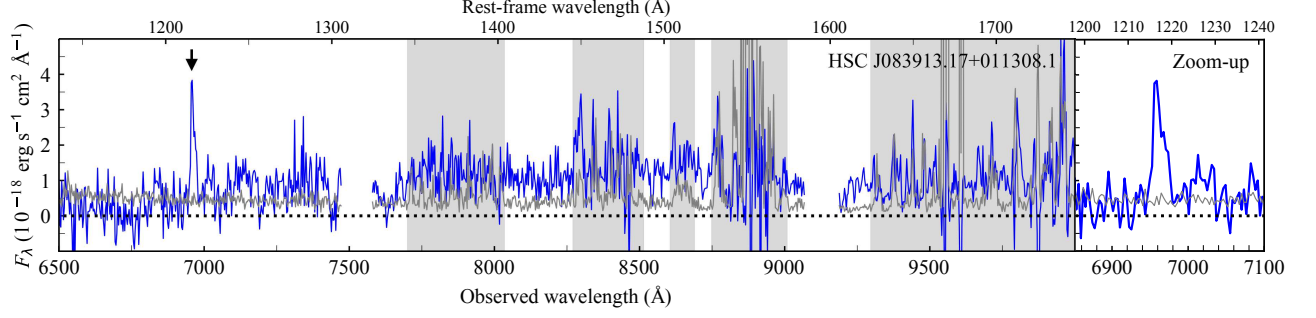


Figure 3. The GMOS spectrum of HSC J0839+0113. The redshifted Ly α to $z = 4.723$ is shown at 6957 Å in the observed-frame (black arrow). Ly α break is also detected at the bluer part than the Ly α line. The full spectrum (blue thin line) and the enlarged spectrum around the Ly α emission line (blue thick line) are shown. A noise spectrum (gray line) serves as a guide to the expected noise. The wavelength regime strongly affected by sky lines are shaded. The missing data points are due to CCD gaps.

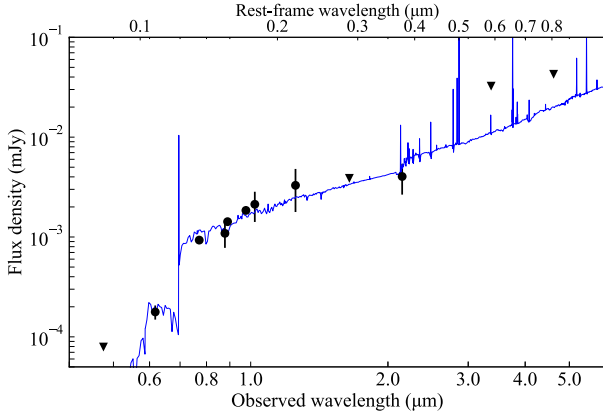


Figure 4. The SED of HSC J0839+0113 and its best fit models. The plotted data are photometries of *grizy* (HSC), *ZYJHKs* (VIKING), and *W1W2* (*WISE*). The circles and triangles denote detections with 1σ error bars and non-detection (3σ upper limits), respectively.

We cross-checked the stellar mass with that estimated with the Mizuki SED template-fitting code (Tanaka 2015), where the Mizuki fitting was performed for all the photometry data of this object. The estimated stellar mass is $11.66^{+0.24}_{-0.26}$. The Mizuki result is consistent with that of CIGALE within the 1σ errors. We do not provide the star formation rate (SFR) from this SED fitting analysis because the SFR is not constrained due to the less number of photometry data in the observed-frame infrared wavelength. The results are further discussed in Section 4.2.

4. DISCUSSION: THE NATURE OF HSC J0839+0113

4.1. Radio Properties

HSC J0839+0113 was selected from Lyman break galaxies (LBGs) with a radio detection of FIRST. Because any criteria on a radio spectral index are not imposed to the selection, discussing its radio prop-

Table 1. Properties of HSC J083913.17 + 011308.1

| | |
|--------------------------------|--|
| R.A., Decl. (J2000) | 08 ^h 39'13''17, +01°13'08''1 |
| Redshift | 4.723 (0.001) |
| r_{AB}, i_{AB} , | 25.66 (0.18), 23.89 (0.03) |
| z_{AB}, y_{AB} | 23.45 (0.04), 23.23 (0.06) |
| Z_{AB}, Y_{AB}, J_{AB} | 23.81 (0.03), 23.1 (0.4), 22.6 (0.5) |
| H_{AB}, K_{SAB} | > 22.4 ^a , 22.4 (0.5) |
| FIRST $S_{1.4\text{GHz}}$ | 7.17 (0.14) mJy |
| GMRT $S_{325\text{MHz}}$ | 36.8 (2.0) mJy |
| TGSS $S_{150\text{MHz}}$ | 54.5 (6.6) mJy |
| $L_{1.4\text{GHz}}$ | $1.63 (0.03) \times 10^{27} \text{ W Hz}^{-1}$ |
| $L_{325\text{MHz}}$ | $8.38 (0.46) \times 10^{27} \text{ W Hz}^{-1}$ |
| $L_{150\text{MHz}}$ | $12.4 (1.5) \times 10^{27} \text{ W Hz}^{-1}$ |
| α_{1400}^{325} | -1.12 (0.02) |
| α_{1400}^{150} | -0.91 (0.02) |
| Ly α flux | $4.3 (0.4) \times 10^{-17} \text{ erg s}^{-1} \text{ cm}^{-2}$ |
| Ly α luminosity | $9.80 (0.10) \times 10^{42} \text{ erg s}^{-1}$ |
| Ly α FWHM | 660 (90) km s ⁻¹ |
| Ly α EW _{rest} | 9.1 (1.6) Å |
| log M_*/M_\odot ^b | 11.43 ($^{+0.22}_{-0.46}$) |

NOTE— 1σ errors are shown in parentheses.

^a 3σ upper limit.

^bThe stellar mass is derived from SED fitting.

erties is relevant. Radio photometric data of HSC J0839+0113 are available in the FIRST 1.4 GHz catalog (Helfand et al. 2015), the 325 MHz GMRT survey catalog in the *Herschel*-ATLAS/GAMA field (Mauch et al. 2013), and the 150 MHz GMRT TGSS Alternative Data Release (Intema et al. 2017).

The spectral indices α ($S_\nu \propto \nu^\alpha$) are calculated to be $\alpha_{1400}^{150} = -0.91 (0.02)$ between 150 MHz and 1.4 GHz,

and $\alpha_{1400}^{325} = -1.12$ (0.02) between 325 MHz and 1.4 GHz, respectively. Alternative spectral index of α_{1400}^{150} is -0.84 in the spectral index catalog by de Gasperin et al. (2018) who re-processed the TGSS and NVSS images. These indices do not meet the criterion defining ultra-steep spectral index, $\alpha < -1.3$ (De Breuck et al. 2000a; Saxena et al. 2018a).

In Figure 5, the spectral index between 325 MHz and 1.4 GHz is shown as a function of redshift together with other known HzRGs. The spectral indices of the other RGs and HzRGs are taken from literature: 3CR (Spinrad et al. 1985), the HzRG sample at $z > 2$ (Miley & De Breuck 2008), the $z = 4.88$ non-USS HzRG with $\alpha = -0.75$ (Jarvis et al. 2009), and the five recently discovered HzRGs at $z > 4$ (α of from -1.34 to -1.64 , Saxena et al. 2019). The spectral indices of the literature samples are calculated between WENSS 325 MHz (Rengelink et al. 1997) and NVSS 1.4 GHz (Condon et al. 1998) or between TEXAS 365 MHz (Douglas et al. 1996) and NVSS 1.4 GHz except for Saxena’s HzRGs. The spectral indices for $z > 4$ Saxena’s HzRGs are calculated between VLA 370 MHz and 1.4 GHz (Saxena et al. 2018a) except for the most distant known HzRG at $z = 5.72$ (TGSS J1530+1049) with a spectral index of -1.4 between TGSS 150 MHz and VLA 1.4 GHz (Saxena et al. 2018b). We can see the $\alpha - z$ correlation at all the redshift range. At $z > 4$, $z = 4.88$ HzRG (J163912.11+405236.5) shows the flattest spectral index. This object has been discovered out of faint mid-infrared sources with a FIRST detection in the *Spitzer*-SWIRE deep field, not by using the USS technique (Jarvis et al. 2009). This is an evident example illustrating non-USS HzRGs at $z > 4$. VLA J1236421+621331, another non-USS HzRG at $z = 4.42$ (Waddington et al. 1999), is not plotted here because the low frequency photometry data is not available. HSC J0839+0113 is located below the $\alpha = -1.3$ selection line (the dotted line in Figure 5), following the $z = 4.88$ HzRG at $z > 4$. HSC J0839+0113 would be never discovered by using the USS technique. This discovery of the non-USS HzRG at $z \sim 5$, along with the previously reported non-USS HzRGs at $z \sim 4 - 5$ (Waddington et al. 1999; Jarvis et al. 2009), suggests that a subset of HzRGs are missed in many USS-based surveys.

The rest-frame radio luminosities of HSC J0839+0113 are $\log L_{1.4\text{GHz}}$ of 27.2 W Hz^{-1} and $\log L_{150\text{MHz}}$ of 28.1 W Hz^{-1} , assuming a mean spectral index, $\alpha = -1.0$, between α_{1400}^{325} and α_{1400}^{150} . Owing to the relatively flat spectrum, the radio luminosities at low frequency is one order of magnitude smaller than those of the previously reported USS-selected HzRGs at $z \sim 4 - 5$, and is a factor of 2–4 smaller than those of the recently reported USS-selected HzRGs at $z \sim 4 - 5$ (Saxena et al. 2019).

4.2. Host galaxy

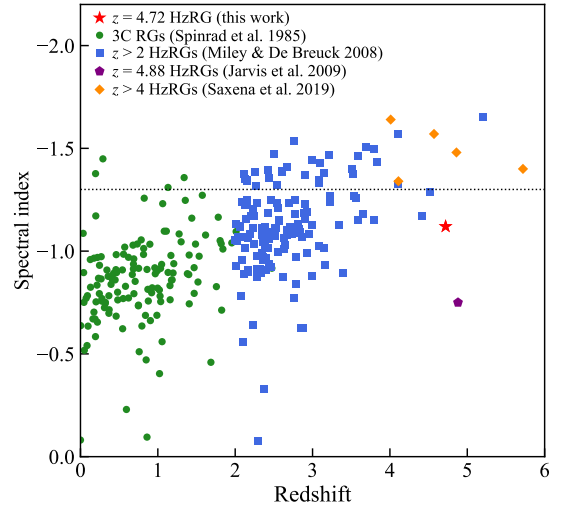


Figure 5. Radio spectral index (α ; $S_\nu \propto \nu^\alpha$) as a function of redshift of RGs. The red star indicates the HSC J0839+0113 in this paper. The known RGs taken from literature are also plotted: 3CR (green circles, Spinrad et al. 1985), the HzRG sample at $z > 2$ (blue squares, Miley & De Breuck 2008), the $z = 4.88$ non-USS HzRG (purple pentagon, Jarvis et al. 2009), and the five recently discovered HzRGs at $z > 4$ (orange diamonds, Saxena et al. 2019). The commonly used criterion of α for USS selection is represented by a dotted line.

HzRGs are often involved with massive hosts ($> 10^{11} M_\odot$, Seymour et al. 2007; De Breuck et al. 2010). We can examine whether HSC J0839+0113 that was selected among LBGs follows the trend or not, using the SED fitting result. The obtained stellar mass of HSC J0839+0113 is $\log M_*/M_\odot = 11.4$ and is as massive as other known HzRGs (Seymour et al. 2007; De Breuck et al. 2010). This massive stellar mass of the host galaxy is supported from a fact that the apparent K_s magnitude of 20.6 Vega mag well follows the $K - z$ correlation for HzRGs, where the correlation is established because of the characteristic massive stellar mass of known HzRGs (e.g., Rocca-Volmerange et al. 2004). HSC J0839+0113, which is a LBG with a radio-AGN, is one of the most massive galaxies among $z \sim 5$ LBGs, which typically have $\log M_*/M_\odot = 8 - 11$ (Yabe et al. 2009). Such a large stellar mass at $z = 4.72$ (at an age of the universe of 1.2 Gyr) suggests that the stellar mass had been rapidly built up through intense star formation. Since HSC J0839+0113 is already very massive at the observed redshift, the star formation should either have been quenched by now or be quenched shortly, and then this HzRG could evolve into a giant elliptical galaxy seen at the present day.

4.3. Ly α Emission

The measured Ly α line flux and luminosity of HSC J0839+0113 are 4.3×10^{-17} erg s $^{-1}$ cm $^{-2}$ and 9.8×10^{42} erg s $^{-1}$, respectively. The underlying continuum is estimated from the continuum of 7000–7300 Å in the spectrum, assuming a flat continuum. Ly α emission is not corrected for extinction. The Ly α luminosity is consistent with those of other $z \sim 4 - 5$ HzRGs (van Breugel et al. 1999; Jarvis et al. 2009; Kopylov et al. 2006; Saxena et al. 2019). The Ly α FWHM is derived with a single Gaussian fitting and is corrected for the instrumental broadening effect. The derived FWHM is 660 km s $^{-1}$. The FWHM is smaller than those of the known HzRGs at $z > 2$, which have typically > 1000 km s $^{-1}$. This narrow FWHM of Ly α could suggest that a dominant ionization source of Ly α of HSC J0839+0113 is neither a broad emission line AGN nor jet-induced shock but star formation or a weak AGN. Saxena et al. (2019) argue that the dominant source of faint HzRGs with low Ly α luminosities ($\sim 10^{43}$ erg s $^{-1}$) and narrow FWHMs (< 600 km s $^{-1}$) at $z > 4$ could be star formation or a weak AGN by compared with Lyman alpha emitters. Our result is not inconsistent with that.

Equivalent width EW_{rest} of Ly α at the rest-frame is calculated to be 9 (1.6) Å from the obtained spectrum. The EW_{rest} of HSC J0839+0113 is much smaller than those of the known HzRGs. The known HzRGs at $2 < z < 4$ show large EW_{rest} of up to ~ 700 Å. For almost all of the HzRGs at $z > 4$, continua are not detected and the upper limits of EW_{rest} are measured to be $> 40 - 180$ Å (De Breuck et al. 2000b; Waddington et al. 1999; Saxena et al. 2018b). The small EW_{rest} of HSC J0839+0113 is probably due to a mixture of its ionization source and optical brightness. UV emission lines of HzRGs are generally explained by photoionization by a powerful AGN and additionally jet-induced shock (e.g., De Breuck et al. 2000b). As discussed above, however, in HSC J0839+0113 the contributions from a powerful AGN or shock must be insignificant. The different ionization source in HSC J0839+0113, therefore, could result in the weak Ly α emission. In addition to the ionization source, the relative bright optical continuum of HSC J0839+0113 ($z_{\text{AB}} = 23.5$) also likely causes the small EW_{rest} . The rest-frame UV continuum emission of HSC J0839+0113 is detected both in HSC and the Gemini spectroscopy, while $z > 4$ HzRGs are not detected (> 23 mag).

A small EW_{rest} is observed as the Ly α deficiency in luminous LBGs (Ando et al. 2006) and is attributed to a dusty absorption in a star-forming galaxy. The obtained small EW_{rest} and the relatively optical brightness indicate its dusty system associated with HSC J0839+0113. This is consistent with the migration on the *riz* diagram in Figure 1 from the model colors of a $z \sim 4.7$ LBG to redder colors which suggests this dusty system. The colors of HSC J0839+0113 cannot be explained by galaxy models with low metallicity, although a low metallic-

ity galaxy at $z \sim 5.2$ could have a similar color to that of HSC J0839+0113. These results support the abundant dust contents in HSC J0839+0113 and suggest the chemically evolved host. Submillimeter continua are detected in approximately half of HzRGs at $2.5 < z < 4$ (Reuland et al. 2004), indicating the presence of dust. Only two $z > 4$ HzRGs (TN J1338-1942 at $z = 4.11$ and TN J0924-2201 at $z = 5.19$) were observed with (sub)millimeter telescopes and their continua were detected (De Breuck et al. 2004; Falkendal et al. 2019). Although these two cases suggest the presence of cold dust there despite their large Ly α EW_{rest} of 200 Å and > 180 Å respectively, however, their Ly α emission are likely powered by a broad emission line AGN or jet-induced shock because of their large Ly α velocity widths of 1000 km s $^{-1}$ and 1500 km s $^{-1}$.

5. SUMMARY

This paper reports the discovery of HSC J0839+0113, a $z = 4.72$ HzRG, in the on-going program to search for HzRGs as part of the Wide and Deep Exploration of Radio Galaxies with Subaru HSC (WERGS) project. HSC J0839+0113 was selected as a HzRG candidate from the HSC data using the Lyman break technique. The redshift was determined with Ly α emission line in the obtained Gemini/GMOS spectrum. From the analyses of the GMOS spectrum and photometric data, we found:

- By the SED fitting with the rest-frame UV-optical photometries, the massive stellar mass of the host galaxy was estimated to be $\log M_*/M_\odot = 11.4$ and is consistent with other known HzRGs but marks one of the most massive galaxies among LBGs at $z = 5$.
- The Ly α line luminosity and FWHM are similar to those of other known $z \sim 4 - 5$ HzRGs. The small EW_{rest} of HSC J0839+0113 is much different from HzRGs at $2 < z < 4$ but consistent with the Ly α deficiency in luminous LBGs, suggesting a dusty host galaxy of HSC J0839+0113. The rest-frame UV colors seen on the *riz* color-color diagram is redder than those of the $z \sim 5$ LBG model and also supports the dusty and chemically evolved host galaxy.
- HSC J0839+0113 has the relatively flat radio spectral index α_{1400}^{325} of -1.1 and thus does not belong to USS HzRGs.

The discovery of HSC J0839+0113 demonstrates the ability of HSC-SSP to find HzRGs without a radio spectral index. A HzRG sample established based on HSC-SSP compensates for a sub-population of HzRGs which are missed in USS selection surveys. Because the HzRG was found out of the pilot selection sample in the early release data of HSC-SSP, the full dataset of HSC-SSP covering 1400 deg 2 has a potential for finding much more

HzRGs at $z > 3$, at which known HzRGs are poor in numbers. HzRGs in our survey will provide a new knowledge on the formation and evolution of massive galaxies and radio-AGNs at the early Universe.

We thank the anonymous referee for the comments that improved this paper. We would like to thank Hiroshi Nagai for useful discussions.

The Hyper Suprime-Cam (HSC) collaboration includes the astronomical communities of Japan and Taiwan, and Princeton University. The HSC instrumentation and software were developed by the National Astronomical Observatory of Japan (NAOJ), the Kavli Institute for the Physics and Mathematics of the Universe (Kavli IPMU), the University of Tokyo, the High Energy Accelerator Research Organization (KEK), the Academia Sinica Institute for Astronomy and Astrophysics in Taiwan (ASIAA), and Princeton University. Funding was contributed by the FIRST program from the Japanese Cabinet Office, the Ministry of Education, Culture, Sports, Science and Technology (MEXT), the Japan Society for the Promotion of Science (JSPS), Japan Science and Technology Agency (JST), the Toray Science Foundation, NAOJ, Kavli IPMU, KEK, ASIAA, and Princeton University.

This paper makes use of software developed for the Large Synoptic Survey Telescope (Jurić et al. 2017; Ivezić et al. 2019). We thank the LSST Project for making their code available as free software at <http://dm.lsst.org>.

This paper is based in part on data collected at the Subaru Telescope and retrieved from the HSC data archive system, which is operated by Subaru Telescope and Astronomy Data Center (ADC) at NAOJ. Data analysis was in part carried out with the cooperation of Center for Computational Astrophysics (CfCA), NAOJ.

The Pan-STARRS1 Surveys (PS1, Chambers et al. 2016; Schlafly et al. 2012; Tonry et al. 2012; Magnier et al. 2013) and the PS1 public science archive have been made possible through contributions by the Institute for Astronomy, the University of Hawaii, the Pan-STARRS Project Office, the Max Planck Society and its participating institutes, the Max Planck Institute for Astronomy, Heidelberg, and the Max Planck Insti-

tute for Extraterrestrial Physics, Garching, The Johns Hopkins University, Durham University, the University of Edinburgh, the Queens University Belfast, the Harvard-Smithsonian Center for Astrophysics, the Las Cumbres Observatory Global Telescope Network Incorporated, the National Central University of Taiwan, the Space Telescope Science Institute, the National Aeronautics and Space Administration under grant No. NNX08AR22G issued through the Planetary Science Division of the NASA Science Mission Directorate, the National Science Foundation grant No. AST-1238877, the University of Maryland, Eotvos Lorand University (ELTE), the Los Alamos National Laboratory, and the Gordon and Betty Moore Foundation.

This study is based on observations obtained at the Gemini Observatory via the time exchange program between Gemini and the Subaru Telescope, processed using the Gemini IRAF package. The Gemini Observatory is operated by the Association of Universities for Research in Astronomy, Inc., under a cooperative agreement with the NSF on behalf of the Gemini partnership: the National Science Foundation (United States), National Research Council (Canada), CONICYT (Chile), Ministerio de Ciencia, Tecnología e Innovación Productiva (Argentina), Ministério da Ciência, Tecnologia e Inovação (Brazil), and Korea Astronomy and Space Science Institute (Republic of Korea).

The National Radio Astronomy Observatory is a facility of the National Science Foundation operated under cooperative agreement by Associated Universities, Inc.

GMRT is run by the National Centre for Radio Astrophysics of the Tata Institute of Fundamental Research.

This research has made use of the Vizier catalogue access tool, CDS, Strasbourg, France.

This work is financially supported by the Japan Society for the Promotion of Science (JSPS) KAKENHI grants: Nos. 16H01101 (TN), 16H03958 (TN), 17H01114 (TN & YO), 17H04830 (YM), 18K13584 (KI), 18J01050 (YT), and 19K14759 (YT). YM acknowledges the support from the Mitsubishi Foundation grant No. 30140.

Facilities: Subaru (HSC), Gemini:South (GMOS), VLA, GMRT,

Software: Python, astropy, Gemini IRAF, CIGALE

REFERENCES

- Abazajian, K., Adelman-McCarthy, J. K., Agüeros, M. A., et al. 2004, *AJ*, 128, 502
- Aihara, H., Arimoto, N., Armstrong, R., et al. 2018a, *PASJ*, 70, S4
- Aihara, H., Armstrong, R., Bickerton, S., et al. 2018b, *PASJ*, 70, S8
- Akiyama, M., He, W., Ikeda, H., et al. 2018, *PASJ*, 70, S34
- Ando, M., Ohta, K., Iwata, I., et al. 2006, *ApJL*, 645, L9
- Bañados, E., Venemans, B. P., Morganson, E., et al. 2015, *ApJ*, 804, 118
- Becker, R. H., White, R. L., & Helfand, D. J. 1995, *ApJ*, 450, 559
- Boquien, M., Burgarella, D., Roehlly, Y., et al. 2019, *A&A*, 622, A103

- Bosch, J., Armstrong, R., Bickerton, S., et al. 2018, *PASJ*, 70, S5
- Bruzual, G., & Charlot, S. 2003, *MNRAS*, 344, 1000
- Burgarella, D., Buat, V., & Iglesias-Páramo, J. 2005, *MNRAS*, 360, 1413
- Calzetti, D., Armus, L., Bohlin, R. C., et al. 2000, *ApJ*, 533, 682
- Carilli, C. L., & Yun, M. S. 1999, *ApJL*, 513, L13
- Chabrier, G. 2003, *PASP*, 115, 763
- Chambers, K. C., Magnier, E. A., Metcalfe, N., et al. 2016, arXiv e-prints, arXiv:1612.05560
- Condon, J. J., Cotton, W. D., Greisen, E. W., et al. 1998, *AJ*, 115, 1693
- Croton, D. J., Springel, V., White, S. D. M., et al. 2006, *MNRAS*, 365, 11
- Cutri, R. M., & et al. 2014, *VizieR Online Data Catalog*, 2328,
- De Breuck, C., van Breugel, W., Röttgering, H. J. A., & Miley, G. 2000a, *A&AS*, 143, 303
- De Breuck, C., Röttgering, H., Miley, G., van Breugel, W., & Best, P. 2000b, *A&A*, 362, 519
- De Breuck, C., Bertoldi, F., Carilli, C., et al. 2004, *A&A*, 424, 1
- De Breuck, C., Seymour, N., Stern, D., et al. 2010, *ApJ*, 725, 36
- de Gasperin, F., Intema, H. T., & Frail, D. A. 2018, *MNRAS*, 474, 5008.
- Douglas, J. N., Bash, F. N., Bozayan, F. A., et al. 1996, *AJ*, 111, 1945
- Dunlop, J. S., & Peacock, J. A. 1990, *MNRAS*, 247, 19
- Edge, A., Sutherland, W., Kuijken, K., et al. 2013, *The Messenger*, 154, 32
- Fabian, A. C. 2012, *ARA&A*, 50, 455
- Falkendal, T., De Breuck, C., Lehnert, M. D., et al. 2019, *A&A*, 621, A27
- Furusawa, H., Koike, M., Takata, T., et al. 2018, *PASJ*, 70, S3
- Harikane, Y., Ouchi, M., Ono, Y., et al. 2018, *PASJ*, 70, S11
- Helfand, D. J., White, R. L., & Becker, R. H. 2015, *ApJ*, 801, 26
- Intema, H. T., Jagannathan, P., Mooley, K. P., & Frail, D. A. 2017, *A&A*, 598, A78
- Ivezić, Ž., Kahn, S. M., Tyson, J. A., et al. 2019, *ApJ*, 873, 111
- Jarvis, M. J., Teimourian, H., Simpson, C., et al. 2009, *MNRAS*, 398, L83
- Jarvis, M. J., & Rawlings, S. 2000, *MNRAS*, 319, 121
- Jarvis, M. J., Rawlings, S., Willott, C. J., et al. 2001, *MNRAS*, 327, 907
- Jurić, M., Kantor, J., Lim, K.-T., et al. 2017, *Astronomical Data Analysis Software and Systems XXV*, 279
- Kawanomoto, S., Uraguchi, F., Komiyama, Y., et al. 2018, *PASJ*, 70, 66
- Klamer, I. J., Ekers, R. D., Bryant, J. J., et al. 2006, *MNRAS*, 371, 852
- Komiyama, Y., Obuchi, Y., Nakaya, H., et al. 2018, *PASJ*, 70, S2
- Kopylov, A. I., Goss, W. M., Pariškiĭ, Y. N., et al. 2006, *Astronomy Letters*, 32, 433
- Madau, P. 1995, *ApJ*, 441, 18
- Madau, P., & Dickinson, M. 2014, *ARA&A*, 52, 415
- Magnier, E. A., Schlafly, E., Finkbeiner, D., et al. 2013, *ApJS*, 205, 20
- Matsuoka, K., Nagao, T., Maiolino, R., et al. 2009, *A&A*, 503, 721
- Matsuoka, Y., Onoue, M., Kashikawa, N., et al. 2016, *ApJ*, 828, 26
- Matsuoka, Y., Onoue, M., Kashikawa, N., et al. 2018a, *PASJ*, 70, S35
- Matsuoka, Y., Iwasawa, K., Onoue, M., et al. 2018b, *ApJS*, 237, 5
- Matsuoka, Y., Onoue, M., Kashikawa, N., et al. 2019, *ApJL*, 872, L2
- Mauch, T., Klöckner, H.-R., Rawlings, S., et al. 2013, *MNRAS*, 435, 650.
- McNamara, B. R., Nulsen, P. E. J., Wise, M. W., et al. 2005, *Nature*, 433, 45
- Miley, G., & De Breuck, C. 2008, *A&A Rv*, 15, 67
- Miyazaki, S., Komiyama, Y., Kawanomoto, S., et al. 2018, *PASJ*, 70, S1
- Morabito, L. K., & Harwood, J. J. 2018, *MNRAS*, 480, 2726
- Morganti, R., Fogasy, J., Paragi, Z., Oosterloo, T., & Orienti, M. 2013, *Science*, 341, 1082
- Nagao, T., Maiolino, R., & Marconi, A. 2006, *A&A*, 447, 863
- Oke, J. B., & Gunn, J. E. 1983, *ApJ*, 266, 713
- Ono, Y., Ouchi, M., Harikane, Y., et al. 2018, *PASJ*, 70, S10
- Overzier, R. A., Miley, G. K., Bouwens, R. J., et al. 2006, *ApJ*, 637, 58
- Pérez-González, P. G., Rieke, G. H., Villar, V., et al. 2008, *ApJ*, 675, 234
- Rengelink, R. B., Tang, Y., de Bruyn, A. G., et al. 1997, *A&AS*, 124, 259
- Reuland, M., Röttgering, H., van Breugel, W., & De Breuck, C. 2004, *MNRAS*, 353, 377
- Rigby, E. E., Argyle, J., Best, P. N., Rosario, D., & Röttgering, H. J. A. 2015, *A&A*, 581, A96
- Rocca-Volmerange, B., Le Borgne, D., De Breuck, C., Fioc, M., & Moy, E. 2004, *A&A*, 415, 931

- Roettgering, H. J. A., van Ojik, R., Miley, G. K., et al. 1997, *A&A*, 326, 505
- Saxena, A., Jagannathan, P., Röttgering, H. J. A., et al. 2018a, *MNRAS*, 475, 5041
- Saxena, A., Marinello, M., Overzier, R. A., et al. 2018b, *MNRAS*, 480, 2733
- Saxena, A., Röttgering, H. J. A., Duncan, K. J., et al. 2019, *MNRAS*, 489, 5053
- Schlafly, E. F., Finkbeiner, D. P., Jurić, M., et al. 2012, *ApJ*, 756, 158
- Schlegel, D. J., Finkbeiner, D. P., & Davis, M. 1998, *ApJ*, 500, 525
- Seymour, N., Stern, D., De Breuck, C., et al. 2007, *ApJS*, 171, 353
- Spinrad, H., Djorgovski, S., Marr, J., et al. 1985, *PASP*, 97, 932
- Steidel, C. C., Gialalisco, M., Pettini, M., Dickinson, M., & Adelberger, K. L. 1996, *ApJL*, 462, L17
- Tanaka, M. 2015, *ApJ*, 801, 20
- Toba, Y., Yamashita, T., Nagao, T., et al. 2019, *ApJS*, 243, 15
- Tonry, J. L., Stubbs, C. W., Lykke, K. R., et al. 2012, *ApJ*, 750, 99
- Toshikawa, J., Uchiyama, H., Kashikawa, N., et al. 2018, *PASJ*, 70, S12
- van Breugel, W., De Breuck, C., Stanford, S. A., et al. 1999, *ApJL*, 518, L61
- Waddington, I., Windhorst, R. A., Cohen, S. H., et al. 1999, *ApJL*, 526, L77
- Wagner, A. Y., & Bicknell, G. V. 2011, *ApJ*, 728, 29
- Yabe, K., Ohta, K., Iwata, I., et al. 2009, *ApJ*, 693, 507
- Yamashita, T., Nagao, T., Akiyama, M., et al. 2018, *ApJ*, 866, 140
- York, D. G., Adelman, J., Anderson, J. E., Jr., et al. 2000, *AJ*, 120, 1579
- Yuan, Z., Wang, J., Zhou, M., & Mao, J. 2016, *ApJ*, 829, 95
- Yuan, Z., Wang, J., Zhou, M., Qin, L., & Mao, J. 2017, *ApJ*, 846, 78